

# Analysis of Penetrators Formed in the Welding Line of Electric-Welded Pipes



Due to the high temperatures involved in the production of electric-welded pipes, reoxidation of steel can promote the formation of particles rich in  $\text{SiO}_2$  and  $\text{MnO}$  along the weld line that are known as “penetrators.” In this work, different pipe samples were analyzed to characterize the typical composition and size of the penetrators found. A methodology was developed to quantify the area occupied by these particles in the fracture surface of Charpy V-Notch test specimens. A relationship was found between the frequency of penetrators and the toughness measured at  $0^\circ\text{C}$ . Additionally, thermodynamic calculations were performed to predict the expected composition of penetrators for different steel compositions. Calculations were compared with measurements carried out in the present work and reported in the literature, showing reasonable agreement.

## Authors

**Constantino Capurro** (top left), Senior Specialist – Steelmaking, Tenaris, Campana, Argentina  
ccapurro@tenaris.com

**Mariano Coloschi** (top right), Senior Researcher – Materials, Tenaris, Campana, Argentina  
mcoloschi@tenaris.com

**Eduardo Martínez**, Department Senior Director – Welding, Tenaris, Campana, Argentina  
eemartinez@tenaris.com

**Martín Valdez** (bottom left), Department Director – Materials, Tenaris, Campana, Argentina  
mavaldez@tenaris.com

**Carlos Cicutti** (bottom right), Department Director – Steelmaking, Tenaris, Campana, Argentina  
ccicutti@tenaris.com

## Introduction

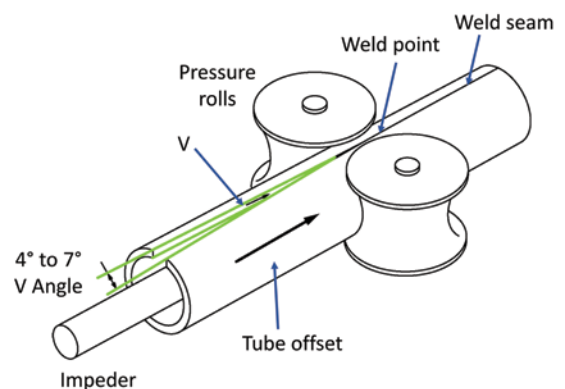
There is an increasing demand for the production of high-quality steels, where the presence of defects and impurities must be minimized. The work carried out by Alan Cramb over several decades has been focused on not only understanding the mechanisms of generation and elimination of nonmetallic inclusions but also on how to transfer these concepts to industrial production.<sup>1</sup> Although inclusions can have different origins, those produced by the reoxidation of steel are of particular importance.<sup>2</sup>

In many cases, these inclusions are formed in the refining and casting stages, especially during transfer operations. However, the same phenomenon can also be present in some subsequent operations, like during the production of electric-welded pipes. To obtain these products, continuous casting slabs are reheated, hot rolled into sheets of different thicknesses and coiled. Then, the

coils are transferred to the pipe mill where they are slitted in strips and passed through a series of forming rolls that progressively convert them into a tubular shape whose edges are joined by electrical welding (Fig. 1). Inadequate control of the main process parameters, such as heat input, welding speed and forging pressure, can lead to the formation of different types of defects.<sup>3–5</sup> Due to the high energy involved, the strip edges melt and nonmetallic oxides are formed by the reaction of liquid steel with air.

Figure 1

Schematic diagram of the electric welding process.



The pressure exerted by the forging rolls promotes the expulsion of a mixture of liquid metal and oxides but, if these oxides are not completely removed, they can remain in the weld line, producing a defect known as “penetrator.” These particles are mainly composed by  $\text{SiO}_2$  and  $\text{MnO}$  and are aligned with the weld line.<sup>3,5–7</sup> Depending on their size and location in the weld, they can severely affect the properties of the joint. It has been shown that the presence of penetrators may deteriorate the toughness,<sup>3,7–9</sup> increase the failure rate during flattening tests<sup>10</sup> or make the material more sensitive to hydrogen-induced cracking.<sup>11</sup>

In the present work, different pipe samples were analyzed to characterize the typical composition and size of the penetrators found. A methodology was developed to quantify the area occupied by these particles in the fracture surface of Charpy V-Notch test specimens. Finally, thermodynamic calculations were carried out to estimate the expected composition of penetrators for different steel chemistries.

## Characterization of Penetrators in the Weld Line

### Materials Analyzed

Several samples of electric-welded pipes that had been rejected due to the presence of penetrators in the welding line were collected for metallographic characterization. All materials studied were low-carbon steels for line pipe applications, typically X52, X60 and X65 grades produced by different steel manufacturers. Table 1 summarizes the typical composition range of the analyzed steels.

### Morphology, Location and Composition of Penetrators

Several cross-sections of the selected pipes were cut and evaluated by optical microscopy. After the penetrators were detected, the samples were etched

with Nital reagent to define the position of the welding line. These analyses confirmed that penetrators were mostly elongated particles located in the weld line with sizes varying from a few microns to several millimeters. Further analysis performed by scanning electron microscopy (SEM)/energy-dispersive x-ray spectroscopy (EDS) indicated that they were mainly composed of  $\text{SiO}_2$  and  $\text{MnO}$  with traces of  $\text{Al}_2\text{O}_3$  (Fig. 2). Different morphologies of penetrators were found in the samples analyzed, as shown in Fig. 3.

Figure 2

Location and composition of penetrators.

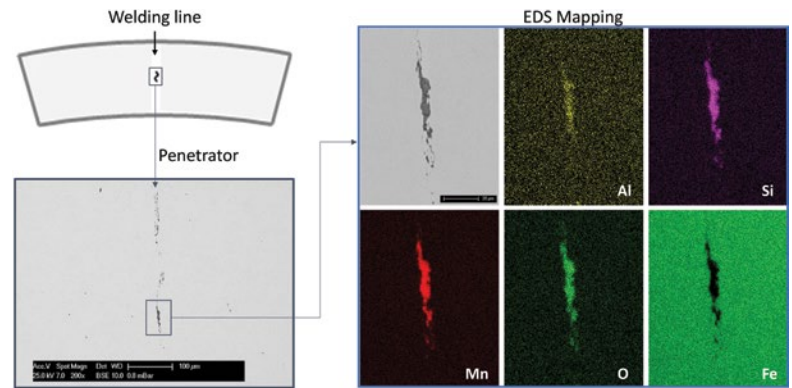


Figure 3

Examples of penetrators found in the samples: isolated particles in the weld plane (a); and large clusters aligned with the weld line (b).

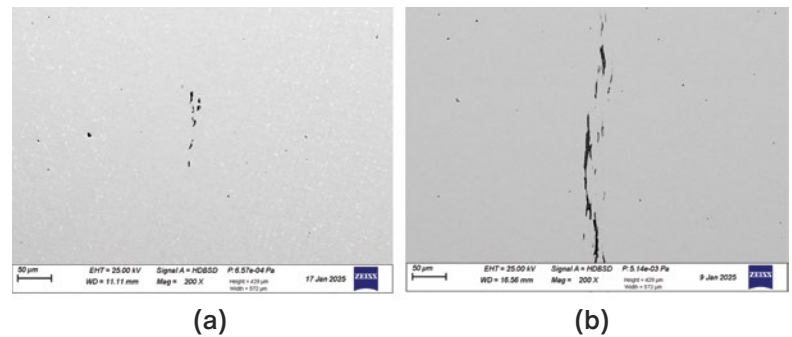


Table 1

Composition Range of the Materials Studied, wt. %

C	Mn	Si	P	S	Al	Ca	Others
0.05 to 0.10	0.80 to 1.60	0.19 to 0.30	0.005 to 0.015	0.001 to 0.002	0.025 to 0.050	0.001 to 0.002	Nb, V, Ti

Figure 4

Location of the different inclusions detected using an automated scanning electron microscopy (SEM)/energy-dispersive x-ray spectroscopy (EDS) analyzer.

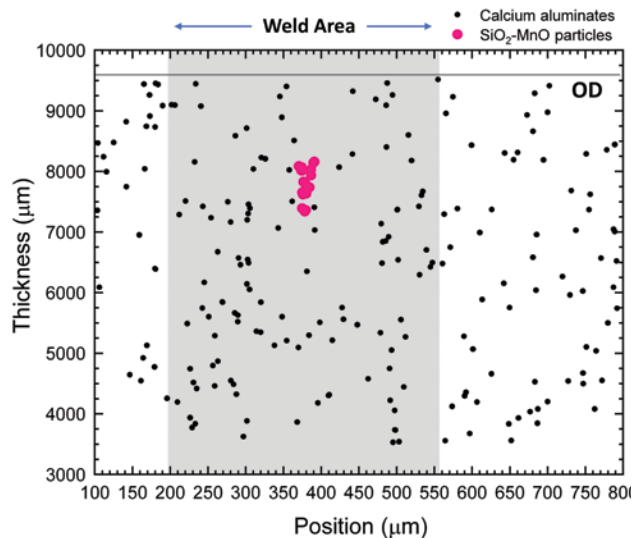


Figure 5

Charpy specimens taken from the welded area.

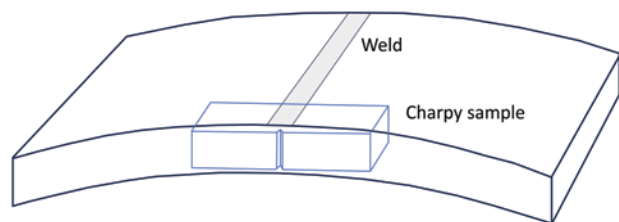
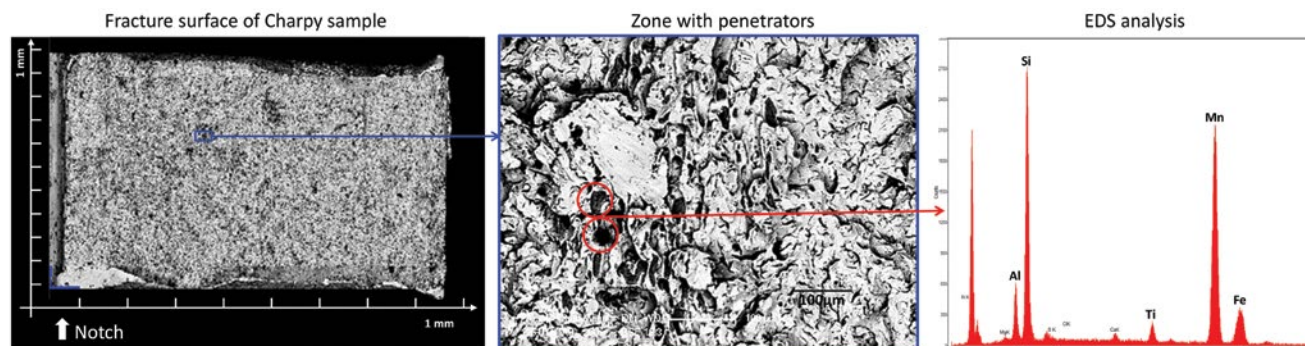


Figure 6

Analysis of Charpy fracture surface by SEM/EDS identifying a region with penetrator.



## Assessment of Penetrators in Charpy Specimens

### Methodology Developed

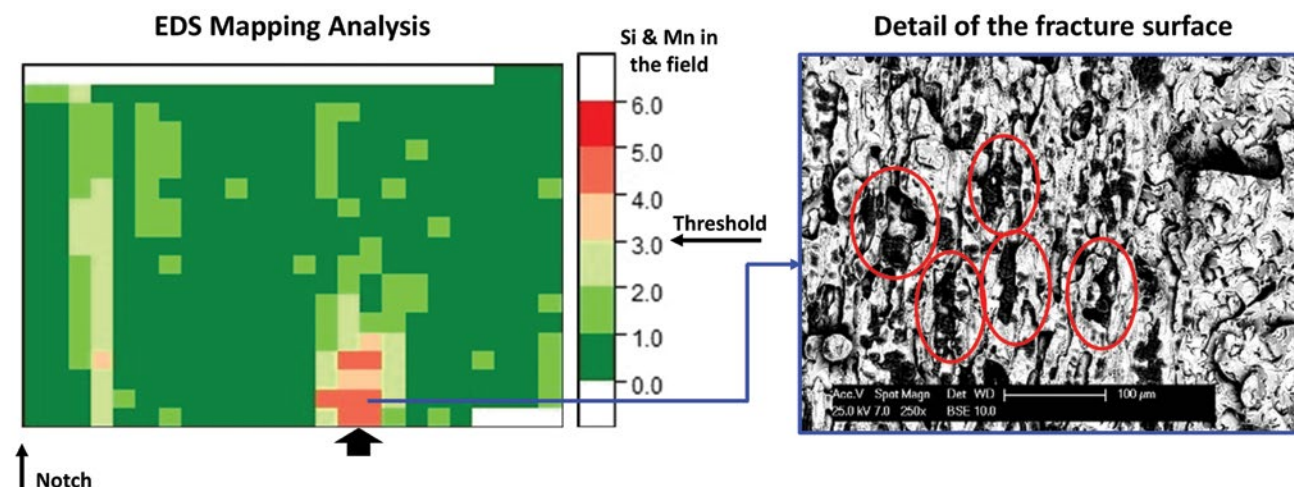
A first attempt was made to quantify the frequency of penetrators using an automatic particle analyzer attached to the SEM, with a methodology similar to that usually applied to evaluate the density of inclusions in lollipop samples.<sup>12</sup> Fig. 4 shows the results obtained in one of the samples analyzed. The procedure can properly differentiate the typical microinclusions present in the base metal (calcium aluminates) from penetrators (rich in  $\text{SiO}_2$  and  $\text{MnO}$ ), which are aligned with the weld line. However, since the frequency of penetrators is relatively low, it is necessary to evaluate a large number of sections to obtain a reliable result.<sup>11</sup>

An alternative method to evaluate the frequency of penetrators in the weld plane was explored.<sup>13</sup> When Charpy V-notch specimens taken from the weld zone are tested (Fig. 5), the fracture surface exposes the plane where the penetrators are usually located. Therefore, penetrators are more likely to be found on this surface than when a cross-section of the pipe is inspected (Fig. 6). One disadvantage is that, since the opened Charpy sample surface is not a flat surface like that obtained in a polished sample, traditional metallographic methods cannot be applied to find the particles.

A methodology based on the analysis by SEM/EDS of the entire fracture surface was implemented. The total area is divided into different fields (typically 1,000 fields for a fracture surface of  $80 \text{ mm}^2$ ) that are automatically scanned and analyzed. As penetrators are mainly composed of  $\text{SiO}_2$  and  $\text{MnO}$ , when the content of Si and/or Mn measured in the field exceeds a threshold value, there is a higher likelihood that the field contains these particles. Threshold levels for Si and Mn are determined by performing EDS analyses in areas free of penetrators.

Figure 7

Procedure developed to detect fields with potential presence of penetrators.



The relationship between the area of the fields with compositions above the threshold and the total surface of the sample can be used as an index to quantify the presence of penetrators in the weld.

The implemented procedure is shown schematically in Fig. 7. After the analysis, a color map is generated with the different Si and Mn contents measured in each field. In this case, there are two zones where the limits are exceeded: one closer to the sample notch and another further away but with a higher concentration. A more detailed SEM analysis of this latter region revealed the presence of numerous penetrators (dark spots in the SEM image). To verify the repeatability of the results, the values obtained from the two halves of the same specimen were compared. Although the fracture of Charpy specimens may leave penetrators on one face and not on the other, in the case of large particles or clusters of smaller particles, it is expected they may remain on both halves. Fig. 8 confirms that there is good agreement in the results obtained for both faces.

### Relationship Between Fracture Toughness and Penetrators Density

Although the fracture toughness of the weld can be affected by different factors, such as the composition of the steel or the heat treatment to which the

joint is subjected,<sup>5,14</sup> the presence of penetrators strongly influences the results obtained.<sup>3,7-9</sup> The procedure described in the previous section was applied to evaluate the frequency of penetrators in 28 specimens that had presented different toughness results in Charpy tests conducted at 0°C. Fig. 9a shows the relationship between the frequency of fields with penetrators and the impact energy measured in each specimen. Despite some dispersion, a deterioration in toughness is observed as the penetrator frequency increases. To evaluate whether not only the frequency but also the position of the penetrators in the section can influence the toughness results, only particles located at a distance less than 2 mm from the specimen

Figure 8

Location of fields with penetrators on both fracture surfaces of the same Charpy specimen.

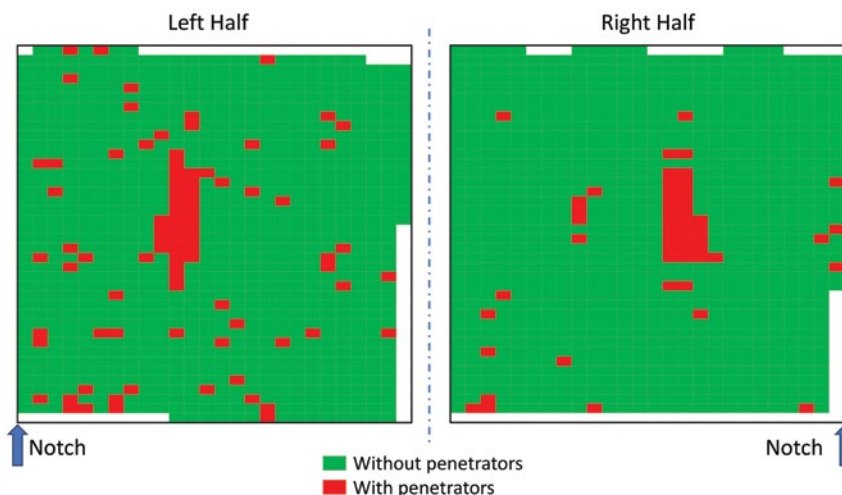
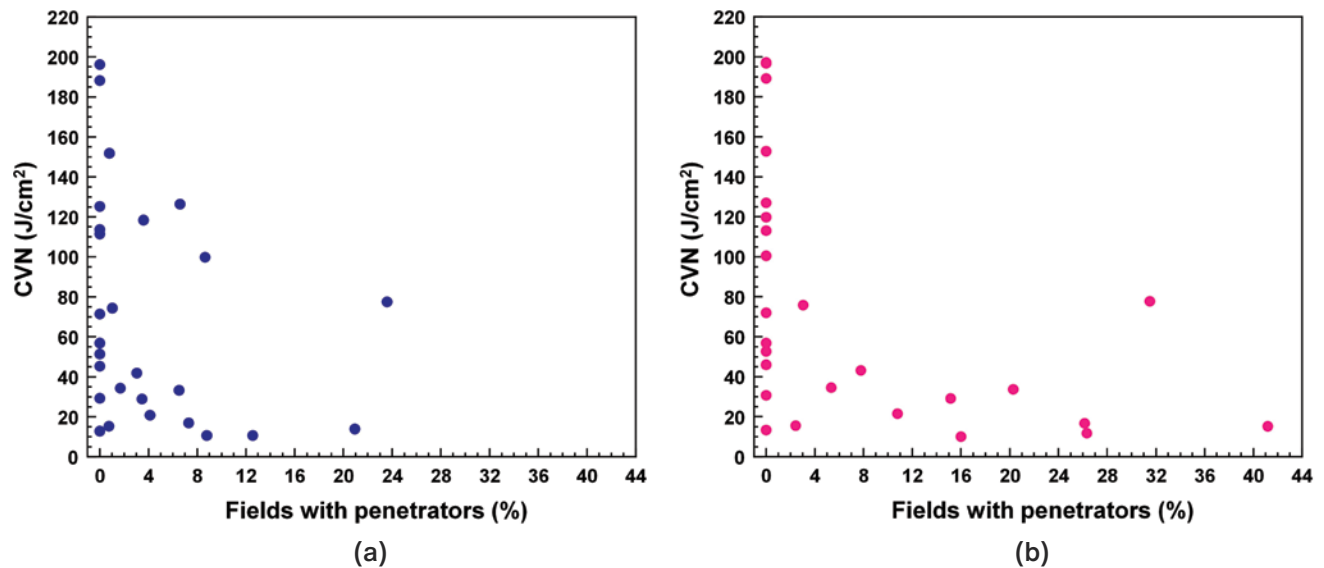


Figure 9

Relationship between the percentage of fields with penetrators and toughness: Whole analyzed area (a) and considering only 2 mm from notch (b).



notch were considered. Results obtained for the same 28 samples are presented in Fig. 9b, where a better correlation with toughness is observed. These findings suggest that the presence of penetrators in regions closer to the notch promotes fracture propagation, thus reducing the energy absorbed during the test.

### Thermodynamic Calculations

Although there are different mechanisms proposed to explain the sequence of stages in which penetrators are formed and removed during the welding process,<sup>3,15,16</sup> it is generally accepted that they originate from the reoxidation of the liquid pool. Among other factors, the

composition of these oxides can affect how easily they can be expelled from the weld during the forming process.<sup>17,18</sup> Therefore, it is important to predict how the composition of the steel may influence the composition of the particles produced.

As described in pioneer studies<sup>19</sup> and confirmed in more recent investigations,<sup>20</sup> the type of inclusions formed during the reoxidation of Al-killed steels will depend on the amount of oxygen picked up by the system. For low oxygen levels, mainly Al<sub>2</sub>O<sub>3</sub> inclusions will be formed. However, as the oxygen content increases, all the available Al will be consumed and the oxidation of Si and Mn present in the steel will continue, generating inclusions with different amounts of Al<sub>2</sub>O<sub>3</sub>, SiO<sub>2</sub> and MnO.

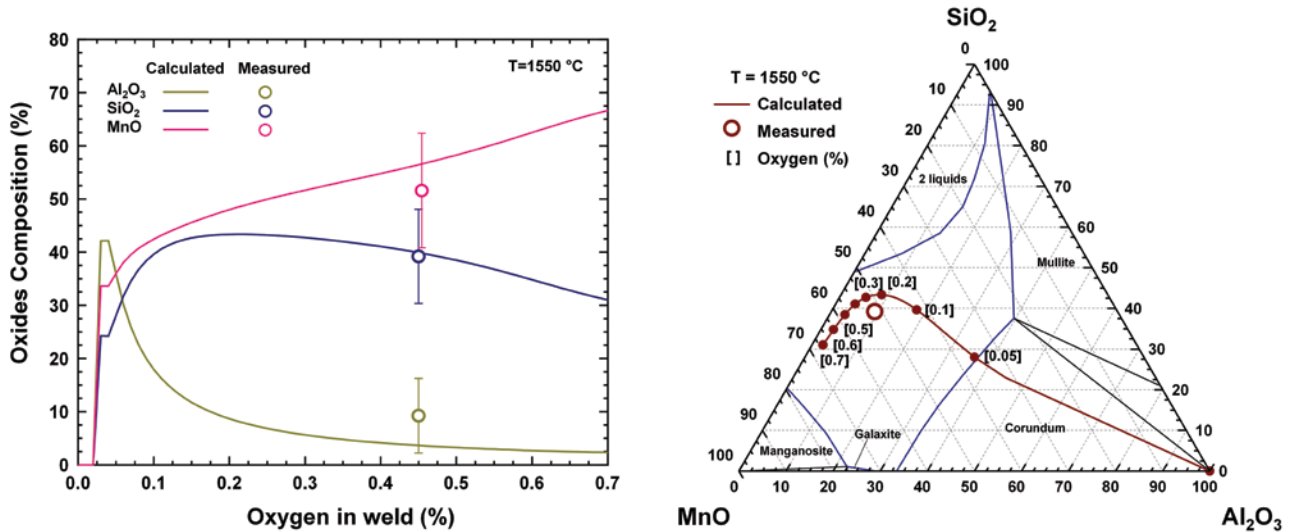
Table 2

#### Steels Selected to Compare the Composition of Penetrators With Simulations

Case	Steel composition (wt. %)					Penetrators' composition (wt. %)		
	C	Mn	Si	Al	Mn/Si	Al <sub>2</sub> O <sub>3</sub>	SiO <sub>2</sub>	MnO
C1	0.08	1.55	0.27	0.023	5.74	9.2 ± 7.0	39.2 ± 8.9	51.6 ± 10.8
C2	0.06	0.87	0.19	0.050	4.58	15.7 ± 4.6	38.5 ± 4.2	45.9 ± 8.0
C3	0.07	1.60	0.30	0.043	5.33	7.9 ± 4.6	37.2 ± 10.4	54.9 ± 10.5
C4	0.08	1.56	0.25	0.039	6.24	9.0 ± 2.3	41.3 ± 5.5	49.7 ± 7.4

Figure 10

Evolution of the calculated inclusion composition for different oxygen contents in steel C1 (see Table 2) together with the penetrator composition measured for this case.

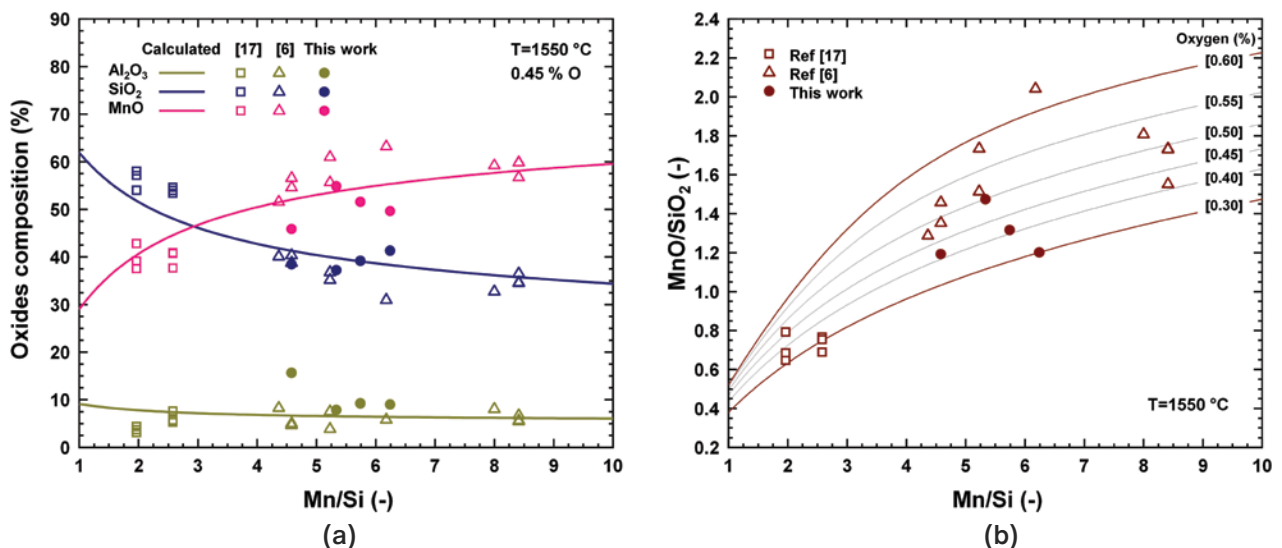


To evaluate the expected composition of the inclusions formed, different simulations were carried out using the commercial package FactSage 7.3. In these calculations, the liquid steel temperature was set at 1,550°C and the oxygen content varied from 0.0 to 1.0%. Different steel compositions were simulated where the penetrators had been characterized by SEM/EDS (see Table 2).

Fig. 10 shows the results obtained for steel C1. As expected, when the oxygen level increases, the Al<sub>2</sub>O<sub>3</sub> content of inclusions decreases and the MnO/SiO<sub>2</sub> ratio increases. The composition of the penetrators observed in the weld line for this steel fits the calculation when the oxygen in the melt is around 0.45%. Additional simulations were performed by fixing the Si content of the steel at 0.25% and varying the Mn level to achieve

Figure 11

Effect of the steel Mn/Si ratio on the composition of penetrators, both measured in this work and reported in the literature:<sup>6,17</sup> Composition changes for a fixed oxygen content (a); and evolution of MnO/SiO<sub>2</sub> ratio for different oxygen contents (b).



Mn/Si ratios from 0 to 10. Calculated values were compared with the composition of penetrators found in the steels shown in Table 2 as well as in different studies published in the literature.<sup>6,17</sup> In general, a reasonable agreement is found between calculated and measured values for the different components (Fig. 11a). The effect of changing the amount of oxygen on the MnO/SiO<sub>2</sub> ratio of the particles is shown in Fig. 11b. Considering oxygen levels between 0.3 and 0.6%, the measured values can be well reproduced.

## Conclusions

Penetrators found in different steels for line pipe applications produced by electric welding process were characterized. In general, these particles are aligned with the

weld line with sizes varying from a few microns to several millimeters and are typically composed of SiO<sub>2</sub>, MnO and traces of Al<sub>2</sub>O<sub>3</sub>. A methodology was developed to assess the area occupied by these oxides on the fracture surface of Charpy test specimens. Analyzing the results of several samples, it was found that the fracture toughness at 0°C decreases when the frequency of penetrators increases. The effect is more noticeable when these particles are located closer to the notch root. Additionally, thermodynamic calculations were performed to estimate the expected composition of penetrators for different steel compositions. Results of these calculations were compared with measurements carried out in the present work and reported in the literature, showing reasonable agreement.

*This article is available online at AIST.org for 30 days following publication.*

## References

1. A. Cramb, "High Purity, Low Residual and Clean Steels," *Impurities in Engineering Materials*, Marcel Dekker Inc., New York, N.Y., USA, 1999, pp. 49–89.
2. Y. Wang, A. Cramb, S. Sridhar, A. Gómez and C. Cicutti, "Re-Oxidation of Low-Carbon Aluminum-Killed Steel," *AIST Transactions*, Vol. 1, No. 2, 2004, pp. 87–96.
3. H. Haga, K. Aoki and T. Sato, "The Mechanisms of Formation of Weld Defects in High-Frequency Electric Resistance Welding," *Welding Journal*, Vol. 60, 1981, pp. 104–109.
4. T. Kyogoku, C. Takamada, K. Hotta, M. Tatsuaki and S. Nemoto, "Automatic Welding Control Weld Tube Mill System for Electric-Resistance Weld Tube Mill," *Transactions ISIJ*, Vol. 24, 1984, pp. 847–856.
5. K. Ravikiran, P. Xu and L. Li, "A Critical Review on High-Frequency Electric-Resistance Welding of Steel Linepipe," *Journal of Manufacturing Processes*, Vol. 124, 2024, pp. 753–777.
6. E. Yokoyama, M. Yamagata, N. Kano and S. Watanabe, "Effects on Penetrator Defect Occurrence of Welding Conditions and Mn/Si Ratio of ERW High Manganese Line Pipe," *Kawasaki Steel Giho*, Vol. 10, No. 1, 1978, pp. 23–33.
7. Y. Matsui, Y. Iizuka, T. Okabe and T. Inoue, "Evaluation Method for Low Temperature Toughness of Weld Seam of HFW Pipe Based on the Distribution of Scattered Type Penetrator," *ISIJ International*, Vol. 57, No. 11, 2017, pp. 2010–2015.
8. T. Tagawa, S. Yamamoto and T. Miyata, "Influence of Weld Oxides on Ductility and Fracture Toughness of Electric Resistance Weld Joint," *Tetsu-to-Hagané*, Vol. 80, No. 4, 1994, pp. 70–75.
9. S. Xu, J. Gianetto, W. Tyson and S. Matsuno, "Toughness of EW Pipe Seam Welds: Fractography and Fracture Path Observations on Charpy V-Notch Impact Specimens From Contemporary Pipe Steels," *Journal of Pipeline Engineering*, Vol. 17, No. 2, 2018, pp. 211–224.
10. K. Babakri, "Improvements in Flattening Test Performance in High Frequency Induction Welded Steel Pipe Mill," *Journal of Materials Processing Technology*, Vol. 210, 2010, pp. 2171–2177.
11. H. Hong, J. Lee and J. Choi, "Improvement of Resistance to Hydrogen Induced Cracking in Electric Resistance Welded Pipes Fabricated With Slit Coils," *Metals and Materials International*, Vol. 15, No. 1, 2009, pp. 133–139.
12. C. Capurro, R. Boeri and C. Cicutti, "Characterization of Non-Metallic Inclusions of Al-Killed Ca-Treated Steels by Automated SEM/EDS and Its Application to Industrial Case Studies," *Steel Research International*, Vol. 93, No. 10, 2022.
13. C. Capurro, M. Coloschi, E. Martínez, M. Valdez and C. Cicutti, "Characterization of Penetrators Formed in the welding line of EW Pipes," *23rd IAS Steel Conference*, 2021, Argentina.
14. M. Coloschi, G. Gómez, M. Valdez, E. Martínez and P. Darcis, "Analysis of Welded Line Pipes Toughness Response to Different Seam Heat Treatments," *Journal of Pipeline Engineering*, Vol. 17, No. 2, 2018, pp. 183–194.
15. J. Choi, Y. Chang, C. Kim, J. Oh and Y. Kim, "Penetrator Formation Mechanisms During High-Frequency Electric Resistance Welding," *Welding Journal*, 2004, pp. 27–31.
16. C. Kim and J. Kim, "The Effect of Electromagnetic Forces on the Penetrator Formation During High-Frequency Electric Resistance Welding," *Journal of Materials Processing Technology*, Vol. 209, 2009, pp. 838–846.
17. S. Watanabe, N. Kano, Y. Hirano, F. Ode and E. Yokoyama, "Recent Progress in Techniques of Manufacturing Small Diameter Electric-Resistance Weld Tubes," *Kawasaki Steel Technical Report*, No. 4, 1981, pp. 84–96.
18. S. Kumar, S. Shukla, S. De, A. Saxena, B. Jha, B. Mishra, A. Verma and S. Mallik, "API X 70 Grade HR Coils for ERW Pipes," *International Journal of Metallurgical Engineering*, Vol. 2, No. 2, 2013, pp. 179–187.
19. J. Farrell, P. Bilek and D. Hilty, "Inclusions Originating From Reoxidation of Liquid Steel," *Electric Furnace Proceedings*, Vol. 28, 1970, pp. 64–86.
20. L. Wang and C. Beckermann, "Prediction of Reoxidation Inclusion Composition in Casting of Steel," *Metallurgical and Materials Transactions B*, Vol. 37B, 2006, pp. 571–588.